Exp.-Nr. **A2-2016-4**
Eingang:
an PAC:

Mainz Microtron MAMI

A2 Collaboration at MAMI

Spokespersons: P. Pedroni, A. Thomas

Proposal for an Experiment

"Measurement of the proton scalar polarizabilities via Compton Scattering"

Spokespersons for the Experiment :
E. J. Downie, D. Hornidge, P. Martel, V. Sokhoyan

Abstract of Physics :
The scalar polarizabilities, α_{E1} and β_{M1}, describe the response of the nucleon to an applied electric or magnetic field, respectively. While the sum is well known via sum rules, the individual values are not as well understood. The magnetic polarizability, β_{M1}, for instance has a relative error of 20%. Experimentally, the polarizabilities are best accessed via Compton scattering, where the cross section is sensitive to β_{M1} at backward angles and the beam asymmetry is sensitive to β_{M1} at forward angles. We propose a measurement of both the cross section and beam asymmetry for Compton scattering below pion photoproduction threshold, allowing a new extraction of the scalar polarizabilities with improved precision.

Abstract of Equipment :
The experiment will be performed at the tagged photon facility of MAMI using the upgraded focal plane detector and the Crystal Ball/TAPS detector setup, along with the PID and MWPC charged particle detectors. The upgraded tagger focal plane will be necessary, with at least one quarter of the focal plane fully instrumented in order for the entire coherent peak to be covered, therefore allowing sufficient control over systematic uncertainties.

MAMI Specifications :

beam energy	883 MeV
beam polarization	unpolarized

Photon Beam Specifications :

tagged energy range	40 – 200 MeV
photon beam polarization	linear (coherent edge ≈130 MeV)

Equipment Specifications :

detectors	Crystal Ball/TAPS, PID, MWPCs
target	Liquid Hydrogen

Beam Time Request :

set-up/test with beam	25 hours
data taking	600 hours

List of participating authors:

- **Institut für Physik, University of Basel, Switzerland**
  S. Abt, S. Garni, M. Günther, A. Käser, B. Krusche, S. Lutterer, M. Oberle, Th. Strub, N.K. Walford, L. Witthauer
- **Institut für Experimentalphysik, University of Bochum, Germany**
  G. Reicherz
- **Helmholtz–Institut für Strahlen- und Kernphysik, University of Bonn, Germany**
  F. Afzal, R. Beck, K. Spieker, A. Thiel
- **JINR, Dubna, Russia**
  N.S. Borisov, A. Lazarev, A. Neganov, Yu.A. Usov
- **SUPA School of Physics, University of Edinburgh, UK**
  M. Bashkanov, S. Kay, D.P. Watts, L. Zana
- **SUPA School of Physics and Astronomy, University of Glasgow, UK**
  J.R.M. Annand, D. Hamilton, D.I. Glazier, S. Gardner, K. Livingston, R.Macrae , I.J.D. MacGregor, C. Mullen, D. Werthmüller
- **Department of Astronomy and Physics, Saint Mary's University Halifax, Canada**
  A.J. Sarty
- **Racah Institute of Physics, Hebrew University of Jerusalem, Israel**
  G. Ron
- **Kent State University, Kent, USA**
  C.S. Akondi, D.M. Manley
- **Institut für Kernphysik, University of Mainz, Germany**
  P. Achenbach, H.J. Arends, M. Biroth, F. Cividini, A. Denig, P. Drexler, M.I. Ferretti-Bondy, W. Gradl, V.L Kashevarov, P.P. Martel, A. Neiser, E. Mornacchi, M. Ostrick, S.N. Prakhov, V. Sokhoyan, C. Sfienti, O. Steffen, M. Thiel, A. Thomas, S. Wagner, J. Wettig, M. Wolfes
- **University of Massachusetts, Amherst, USA**
  R.Miskimen, A. Rajabi
- **Institute for Nuclear Research, Moscow, Russia**
  G. Gurevic, R. Kondratiev, V. Lisin, A. Polonski
- **INFN Sezione di Pavia, Pavia, Italy**
  A. Braghieri, S. Costanza, P. Pedroni
- **Department of Physics, University of Regina, Canada**
  Z. Ahmed, G.M. Huber, D. Paudyal
- **Mount Allison University, Sackville, Canada**
  D. Hornidge
- **Tomsk Polytechnic University, Tomsk, Russia**
  A. Fix
- **George Washington University, Washington, USA**
  W.J. Briscoe, C. Collicott, E.J. Downie, I.I. Strakovski

- **Rudjer Boskovic Institute, Zagreb, Croatia**
  M. Korolija, I. Supek

1 Introduction

In 2010, a groundbreaking measurement of $2S$–$2P$ transitions in muonic hydrogen (μH) [1] introduced the "proton radius puzzle," which has become one of the largest open questions in contemporary hadronic, nuclear, and precision atomic physics [2, 3]. Five years after the first μH experiment, we still do not know what is responsible for the (7σ) discrepancy in the proton charge radius seen in μH versus the normal hydrogen (H) and elastic ep scattering. Possible explanations include the effects of proton structure other than the charge radius, namely the higher moments of the proton charge and magnetization distributions and, of course, the polarizabilities. The proton polarizability effects [4–6] appear rather prominently in μH, while being highly suppressed in H (by the electron-muon mass ratio) [7].

The muonic-atom spectroscopy program at Paul Scherrer Institute in Switzerland continues with the measurements of muonic deuterium [8], tritium, and helium. The polarizabilities of the nucleon, as well as of the few-nucleon systems, play a crucial role in the interpretation of these experiments, and are presently at the precision frontier. Here we propose to provide a high-precision measurement of the proton scalar polarizabilities.

The concept of polarizabilities is well known from classical electrodynamics. In the presence of an external e.m. field, a system with an intrinsic distribution of electric charge and magnetism acquires the induced dipole moments. The size and direction of these are given by the polarizabilities. For a classical point-like charge or magnetic monopole the polarizabilities are zero by definition. The pion and the nucleon, on the other hand, have a composite structure resulting in non-vanishing polarizabilities. The Lorentz and discrete symmetries constrain such a response for a spinless object (e.g., pion) to two independent scalar polarizabilities: electric and magnetic, denoted as α_{E1} and β_{M1}. The nucleon, having spin-1/2, has, in addition to the scalar polarizabilities, four spin (or vector) polarizabilities denoted by $\gamma_{E1E1}, \gamma_{M1M1}, \gamma_{M1E2}, \gamma_{E1M2}$. The nucleon polarizabilities

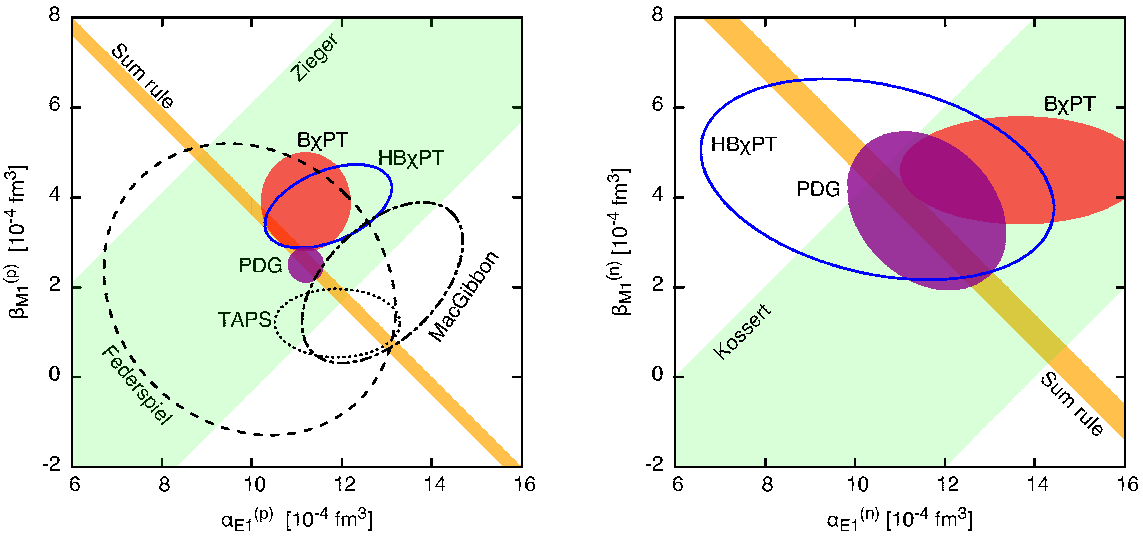

Figure 1: The scalar polarizabilities, β_{M1} versus α_{E1} for the proton (left) and neutron (right). "Sum rule" indicates the Baldin sum rule constraint. "PDG" represents the latest Particle Data Group value [14]. The covariant baryon chiral perturbation theory (BChPT) prediction [15] is shown by the red blob.

are accessed in the process of Compton scattering off the nucleon. The scalar polarizabilities appear in the effective interaction Hamiltonian for real Compton scattering at second order in photon energy

$$H_{\rm eff}^{(2)} = -4\pi \left[\frac{1}{2}\alpha_{E1}\vec{E}^2 + \frac{1}{2}\beta_{M1}\vec{H}^2 \right],$$

and describe the response of the nucleon's internal structure to an external electric or magnetic field, whereas the spin polarizabilities enter at third order:

$$H_{\rm eff}^{(3)} = -4\pi \left[\frac{1}{2}\gamma_{E1E1}\vec{\sigma}\cdot(\vec{E}\times\dot{\vec{E}}) + \frac{1}{2}\gamma_{M1M1}\vec{\sigma}\cdot(\vec{H}\times\dot{\vec{H}}) - \gamma_{M1E2}E_{ij}\sigma_i H_j + \gamma_{E1M2}H_{ij}\sigma_i E_j \right].$$

A number of Compton scattering experiments have been performed (e.g., [9–13]) yielding the scalar polarizabilities of the proton and neutron shown in Fig. 1. The purple region therein represents the Particle Data Group (PDG) average of the empirical extractions of polarizabilities from the experimental data. One can see that the proton polarizabilities presently have an order of magnitude smaller uncertainty than those of the neutron. Figure 2 shows the proton results for the sum of the polarizabilities (left panel) and

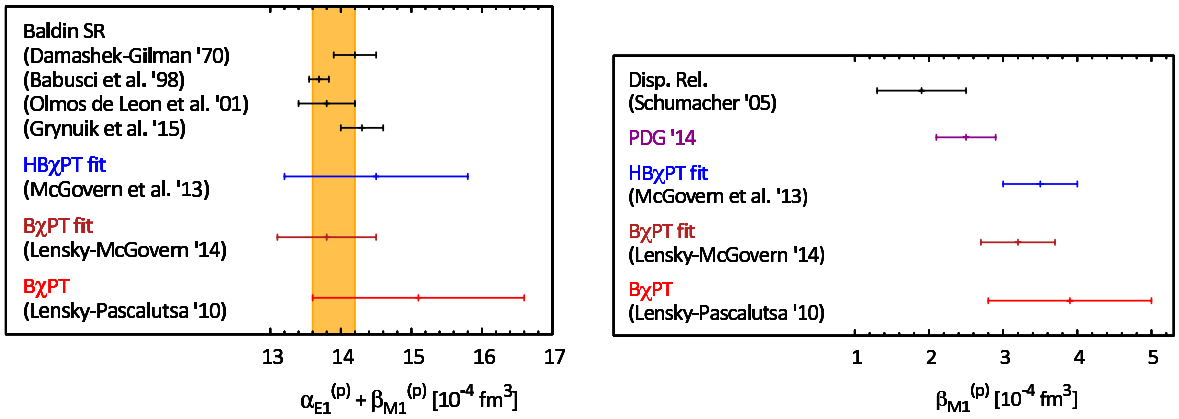

Figure 2: Calculations and empirical extractions for $\alpha_{E1}+\beta_{M1}$ (left) and β_{M1} (right) for the proton. The orange band is the Baldin sum rule.

the magnetic polarizability (right panel). Until 2013, the proton magnetic polarizability showed a significant (2 to 3 σ) discrepancy between the PDG value and the result of chiral perturbation theory (ChPT). The 2013 online edition and the 2014 published edition of the PDG Tables have a new value, shown in the figure, which includes a ChPT based extraction. The discrepancy of ChPT results with some earlier extraction based on dispersive modeling still remains. We propose to carry out a new experimental measurement of the proton scalar polarizabilities by measuring the unpolarized cross section for Compton scattering combined with an alternative technique, whereby polarizabilities are separately extracted from beam polarization data rather than jointly by fitting the angular distributions of the unpolarized cross section.

The main idea and motivation to measure the proton scalar polarizabilities has already been presented to the PAC 2012 (E. J. Downie et al., MAMI-A2/06-2012). The proposal was rated with A, and 750 hours of beamtime were recommended to perform the corresponding measurements with the Crystal Ball/TAPS experiment at MAMI. A

single 300-hour measurement was performed in June 2013, and the results are summarized in [17]. The experiment clearly provided proof-of-principle that the scalar polarizabilities can be accessed in this way. However, with less than half of the proposed time, and an unexpected low-energy background—later identified as coming from beam-dump neutrons—the experiment could not provide a high-precision extraction. With the advent of the upgraded tagger, the rate at which the experiment can take data is substantially increased, the backgrounds are now fully characterized and understood, and it therefore makes sense to revisit the proposal with updated plans based on the valuable experience of 2013 and the analysis thereof.

This proposal utilizes the same motivation to measure the proton scalar polarizabilities α_{E1} and β_{M1}, and aims to achieve unprecedented high precision in the determination of these quantities using the results and experience acquired since 2013. In the next sections, we present the plan of a new high-precision measurement of the unpolarized cross section ($d\sigma/d\Omega$) and beam asymmetry (Σ_3) for Compton scattering off the proton. This will lead to the extraction of the proton scalar polarizabilities with unprecedentedly high precision from a single experiment. In order to obtain realistic estimates based on the performance of the available detector system, we will use data from the pilot experiment performed in June 2013. Furthermore, we use new theoretical calculations and fits of the experimental data within Baryon Chiral Perturbation Theory (BChPT), Heavy Baryon Chiral Perturbation Theory (HBChPT), and Dispersion Relations (DR) in order to estimate the sensitivity of the unpolarized cross section and beam asymmetry to the scalar polarizabilities of the proton.

2 Expected data quality

2.1 Feasibility of the experiment

A pilot experiment for measuring the quantities α_{E1} and β_{M1} was performed in June 2013. A beam of linearly polarized photons impinged on a 10-cm liquid hydrogen target. The experiment used the standard A2 setup of the Crystal Ball (CB) and TAPS, as described in appendices A.2 and A.3. This included charged particle identification which, in the CB region of $30^\circ < \theta < 155^\circ$, is based on the Multiwire Proportional Chambers (MWPCs) and the Particle Identification Detector (PID). A reasonably clean data sample of more than 200,000 Compton scattering events was obtained in the energy range of $E_\gamma = 76-139\,\mathrm{MeV}$ and angular range of the CB. The very forward angles were not analyzed due to significant contamination from electromagnetic background. The overall background contamination in the range used to extract the unpolarized cross section and beam asymmetry did not exceed 4% (being somewhat higher in the forward direction), after all cuts are made. An example for the missing mass spectrum is shown in Figure 3, illustrating good agreement between unpolarized (ϕ-integrated) components for the two linear polarization settings used in the experiment (the polarization plane of one is rotated by 90° with respect to the other). The experimental data are also in good agreement with the result of Monte Carlo simulation.

While the main goal of this experiment was to measure the beam asymmetry, preliminary unpolarized cross sections were additionally extracted in order to control the systematic effects in the data and to estimate the impact of the data on the extraction

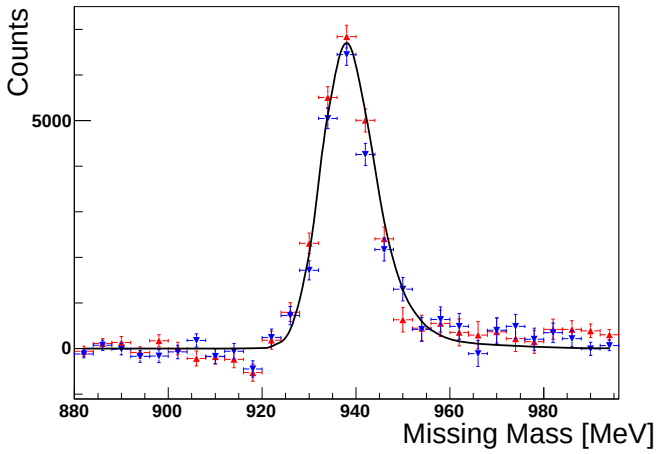

Figure 3: Missing mass spectrum for the energy range 76–98 MeV and $30° < \theta < 155°$, for two settings of the polarization plane with an offset of 90° (blue and red). The black curve shows the corresponding simulated Monte Carlo distribution.

of the proton scalar polarizabilities. In the pilot experiment (June 2013) the positioning of the diamond radiator suffered from instabilities which, due to the nature of coherent Bremsstrahlung, led to time dependent variations of the incident photon energy spectrum, particularly in the region of the linear polarization peak. This fact led to an $15 - 20\%$ systematic error due to flux normalization. Despite this, these preliminary results on the unpolarized cross sections are found to be in reasonable agreement with the data extracted previously by Olmos et al. [12] at MAMI. Figure 4 shows the comparison of the new data (blue), where the results obtained with both polarizations were summed together, with the measurements performed at MAMI using the TAPS setup (red). Overall the sizes of the statistical errors are compatible between both data sets, although in the region where the linear polarization peak was set, the new data show smaller statistical errors. In Figure 4, the data are also compared to three theoretical calculations: DR, BChPT, and HBChPT ($\alpha_{E1} = 10.65 \times 10^{-4}\,\mathrm{fm}^3$ and $\beta_{M1} = 3.15 \times 10^{-4}\,\mathrm{fm}^3$).

The idea to measure the beam asymmetry was based on the calculations presented in [16] where this observable was shown to provide an alternative approach to access proton scalar polarizabilities. Figure 5 (left) shows the corresponding experimental results, that are compared to the theoretical calculations and to the Born terms, which do not include any proton polarizability terms.

The experiment showed that the extraction of Σ_3 for Compton scattering is feasible. The data are in good agreement with BChPT, HBChPT and DR calculations (practically overlapping in Fig. 5) and deviates notably from the Born term that does not depend on the scalar polarizabilities of the proton. The impact of the data was estimated with BChPT and HBChPT and will be published in [17]. A preliminary extraction of the polarizabilities, through fitting the unpolarized cross section and beam asymmetry within the BChPT framework, gives $\alpha_{E1} = 10.8 \pm 1.1 \times 10^{-4}\,\mathrm{fm}^3$ and $\beta_{M1} = 2.9 \pm 1.1 \times 10^{-4}\,\mathrm{fm}^3$.

In summary, the pilot experiment served as a proof of principle, demonstrating the feasibility of measuring the beam asymmetry and unpolarized cross sections with the CB/TAPS setup at MAMI in order to extract the proton scalar polarizabilities. The

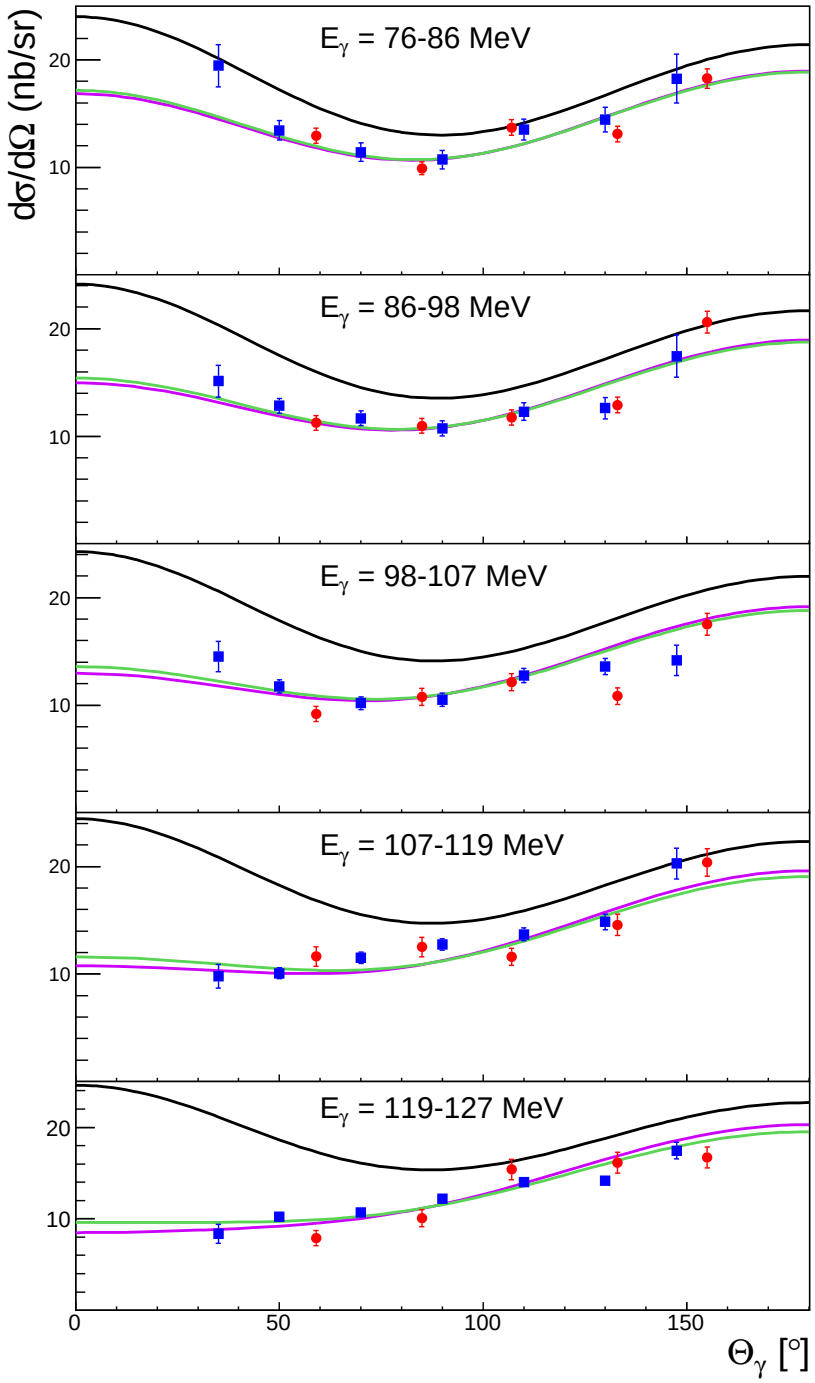

Figure 4: Differential cross sections of Compton scattering, blue: June 2013 data from the pilot experiment, red: previous data [12], violet: DR prediction, green: BChPT, (both DR and BChPT obtained with $\alpha_{E1} = 10.65 \times 10^{-4}\,\mathrm{fm}^3$ and $\beta_{M1} = 3.15 \times 10^{-4}\,\mathrm{fm}^3$), black: Born contribution.

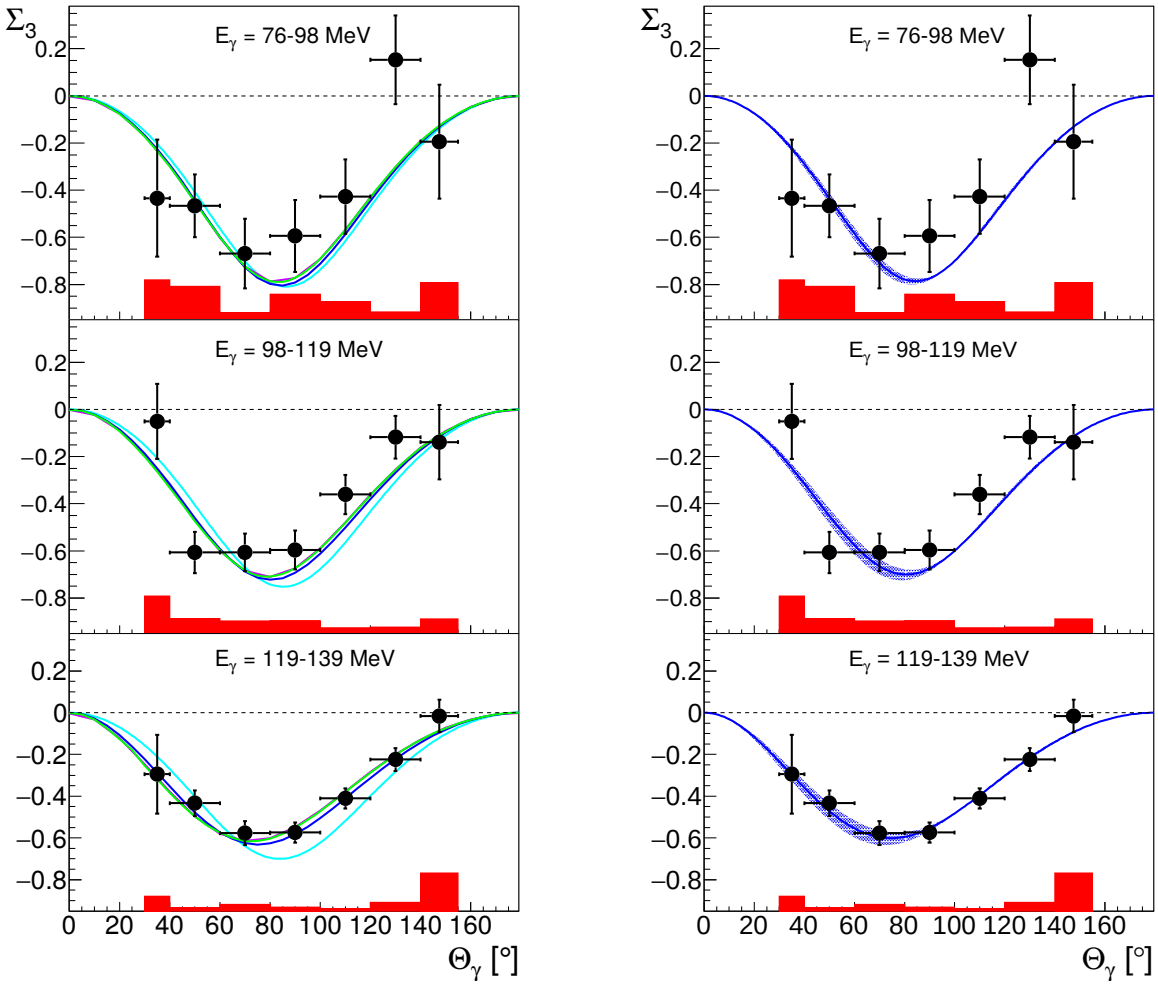

Figure 5: Left panel: Beam asymmetry for three energy ranges (uppermost: $76-98$ MeV, middle: $98-119$ MeV, lowermost: $119-139$ MeV). The errors represent statistical errors, the red bars indicate the systematic error. Green curve: BChPT calculation [15], magenta: DR calculation [19, 20], blue: HBChPT [21], all with $\alpha_{E1} = 10.65 \times 10^{-4}\,\mathrm{fm}^3$ and $\beta_{M1} = 3.15 \times 10^{-4}\,\mathrm{fm}^3$; turquoise: Born term. Right panel: The result of the fit within BChPT framework (blue curve). Shaded bands are determined by the error in β_{M1}.

	Diamond (both settings)		Copper radiator	
Experiment	Full target	Empty target	Full target	Empty target
Pilot	116 hours	110 hours	42 hours	39 hours
Proposed	500 hours	70 hours	30 hours	-

Table 1: Distribution of the time for different radiators and targets in the pilot and planned experiments.

cross sections were obtained with overall compatible statistics compared to the previously existing data, providing higher accuracy in the region around $E_\gamma = 130\,\mathrm{MeV}$. Also, the angular coverage was extended in the forward direction (see Fig. 4). The beam asymmetry was extracted for the first time below pion production threshold and showed sensitivity to dynamical effects which include (among other quantities) the scalar polarizabilities of the proton.

2.2 Optimization of the run conditions and experimental setup

The pilot experiment described above allowed us to prove that a high precision measurement of the scalar polarizabilities is feasible. However, in order to achieve a noticeable improvement in the extraction of the proton scalar polarizabilities, significant improvement needs to be made in the sizes of the statistical errors. The pilot experiment was composed of 116 hours of data with the hydrogen target, as well as 110 hours of data with the empty target, both of which used the diamond radiator, giving equal time between the two diamond orientations. Also, in order to understand the systematic effects and determine the degree of linear polarization of the photon beam a 10 μm Cu radiator was used for an additional 42 hours of data with the hydrogen target and 39 hours with the empty target, as summarized in Table 1.

While the proposed experiment has an extended measurement period that alone would be nearly twice the data of the pilot experiment, there are three major additional factors that will allow for a significant improvement of the Compton scattering statistics.

Firstly, the ratio between the data taken with the full and empty targets was chosen such that the empty target contributions in the full target spectra would be described reasonably well in order to avoid artificial structures introduced through the normalization and subtraction of the empty target data. The shapes of the unpolarized component and of the phi-distributions show that the time taken with the empty target is already sufficient and does not require further extension.

Secondly, the ratio of the Cu data compared to the diamond data, chosen to be $\approx 1:4$, has been found to be unnecessarily high. The analysis of the acquired data indicates that a ratio of 1:20 is sufficient for precise determination of the degree of linear polarization of the photon beam. Combining these two factors, approximately four times higher statistics can be achieved with the proposed measurement time of 600 hours.

Thirdly, in the experiment performed in June 2013 the limit for the event rate was determined by the performance of the tagging system. The upgraded tagger, the first tests of which are already planned for December 2016, is expected to withstand about five times higher beam currents. This is due to two improvements: removing the overlap between channels which allows for a factor of two increase, and using improved detectors and electronics which allows for a factor of 2.5 increase. This factor of five, combined

with the factor of four from the increased and optimized beam time, gives a factor of 20 improvement to the statistics. However, the second of the tagger improvements does come with the caveat that a higher rate in a given tagger channel results in a larger background due to random coincidences. In the pilot experiment the random background was $\approx 50\%$ of the overall signal, giving a 1:1 ratio of prompt to random events. With this second increase in each tagger channel by a factor of 2.5, the prompt to random event ratio will become 2:5. This means that although the statistics will improve by a factor of 20, the relative error will not be reduced by $\sqrt{20} \approx 4.5$, but rather by ≈ 3.5. Such an improvement, combined with the pilot data set as well as previous data sets, will make a marked improvement in the extraction of the scalar polarizabilities.

The analysis shows that we can also expect a compatible reduction of the systematic (and thus combined) error in the final data sample. The main sources of the systematic error are listed below:

a) The main source of the error, particularly for the unpolarized (absolute) cross section in the pilot experiment was due to the normalization with the photon flux. The more reliable tagger and the availability of the pair spectrometer in the data will allow for better tracking of the tagging efficiency, which measures the ratio of photons on target to electrons in the tagger, over time. Additionally, this will reduce the frequency with which these efficiencies need to be performed, as opposed to the daily runs taken during the pilot experiment. Furthermore, the stable function of the goniometer setup will allow us to determine the flux with significantly higher precision.

b) The improved flux normalization will in turn affect the empty target background subtraction procedure, leading to smaller background contamination and respective reduction of the systematic error.

c) The variation in the degree of polarization of the photon beam (important only for the beam asymmetry) is reduced significantly with the current setup. The application of the well-understood method of the event-based determination of the degree of linear polarization will allow us to determine the polarization degree with negligibly small error.

d) The availability of higher statistics in the new data sample will allow us to achieve better fits of the azimuthal angular distributions, thus allowing the determination of the possible phase shifts (due to positioning of the diamond) with higher precision.

3 Expected precision and beam time estimate

As mentioned above, the goal of this experiment is to achieve unprecedented high precision in the determination of the scalar polarizabilities of the proton. The combination of factors mentioned in the previous section leads to the reduction of the overall error by a factor of ≈ 3.5. We used this factor in order to estimate precision of the extraction of the scalar polarizabilities in the new experiment.

Both analyses performed within BChPT and HBChPT frameworks show that the error in the determination of the magnetic polarizability β_{M1} scales linearly with the size of the error of the unpolarized cross section or beam asymmetry used as input.

			Errors from ChPT fit ($10^{-4}\,\mathrm{fm}^3$)					
			With Baldin			Without Baldin		
Experiment	Compton events		Σ_3	$\frac{d\sigma}{d\omega}$	Σ_3, $\frac{d\sigma}{d\omega}$	Σ_3	$\frac{d\sigma}{d\omega}$	Σ_3, $\frac{d\sigma}{d\omega}$
Pilot	$\approx 200,000$	$\Delta\alpha_{E1} \approx$	2.5	1.3	1.1	3.8	1.4	1.3
		$\Delta\beta_{M1} \approx$				2.5	1.7	1.4
Proposed	$\approx 4,000,000$	$\Delta\alpha_{E1} \approx$	0.7	0.4	0.3	1.1	0.4	0.4
		$\Delta\beta_{M1} \approx$				0.7	0.5	0.4

Table 2: Achieved precision in the pilot experiment and expected precision in the proposed experiment for α_{E1} and β_{M1}. When constrained with the Baldin sum rule, the errors on α_{E1} and β_{M1} are roughly identical, hence the quote of a single number.

Thus, the reduction of ≈ 3.5 in the size of the error would lead to the corresponding reduction of ≈ 3.5 in the determination of the error of β_{M1}. The results of the fit of the available data (June 2013) and expected precision in the proposed experiment is summarized in Table 2. As becomes clear from these numbers, the precision in the determination of $\Delta\alpha_{E1} \approx \Delta\beta_{M1} = 0.4 \times 10^{-4}\,\mathrm{fm}^3$ provided by the Particle Data Group extracted from various data sets and theoretical calculations (leading to double counting of the experimentally obtained points) can be improved based on a single measurement.

The comparison of the cross section extracted from the data acquired in the pilot experiment with the previously published highest statistics data set (Olmos et al.) shows that the new data exceeds the previous data set by $\approx 30\%$ *, additionally providing acceptance extension in the forward direction. With application of the Baldin sum rule the previous data set (Olmos et al.) alone led to the result $\alpha_{E1} = 12.1 \pm 1.08 \times 10^{-4}\,\mathrm{fm}^3$ and $\beta_{M1} = 1.6 \pm 0.89 \times 10^{-4}\,\mathrm{fm}^3$ (Baldin sum rule is applied, the error represents the combination of the statistical and systematic errors). Since the data acquired by Olmos et al. constitutes $\approx 50\%$ of the existing world data, the influence of the addition of the other experimental sets (without double counting) can be roughly estimated as $\Delta\alpha_{E1} \approx \frac{1.08}{\sqrt{2}} = 0.76 \times 10^{-4}\,\mathrm{fm}^3$ and $\Delta\beta_{M1} \approx \frac{0.89}{\sqrt{2}} = 0.62 \times 10^{-4}\,\mathrm{fm}^3$. Thus, the errors of $\Delta\alpha_{E1} \approx \Delta\beta_{M1} = 0.3 \times 10^{-4}\,\mathrm{fm}^3$ (with Baldin sum rule constraint) expected in the new experiment will overcome the results obtained directly from the existing experimental data on Compton scattering. As shown in Table 2, the results without application of the Baldin sum rule, also allow for a significant improvement in the determination of α_{E1} and β_{M1}.

In summary, we propose a high-precision measurement of the scalar dipole polarizabilities of the proton. The new data set on unpolarized cross section and beam asymmetry for Compton scattering off the proton, measured mainly below pion production threshold, will allow us to extract the proton scalar polarizabilities α_{E1} and β_{M1} with unprecedented precision based on one single measurement. The feasibility of this experiment has already been proven in the pilot experiment (June 2013), and the systematic effects are well-controlled and understood. The theoretical calculations and fits of the available data within BChPT and HBChPT confirm that the new data will have an essential impact on the determination of α_{E1} and β_{M1}.

*Note that only the part below pion production threshold was used for fitting the new data.

References

[1] A. Antognini, F. Nez, K. Schuhmann, *et al.*, Science **339**, 417 (2013).

[2] J. C. Bernauer and R. Pohl, "The proton radius problem," Sci. Am. **310**, no. 2, 18 (2014).

[3] C. E. Carlson, Prog. Part. Nucl. Phys. (to appear), arXiv:1502.05314 [hep-ph].

[4] S. D. Drell, J. D. Sullivan, Phys. Rev. **154**, 1477 (1967).

[5] J. Bernabeu, T. E. O. Ericson, Z. Phys. A **309**, 213 (1983).

[6] R. N. Faustov, A. P. Martynenko, Phys. Atom. Nucl. **63**, 845 (2000); A. P. Martynenko, Phys. Atom. Nucl. **69**, 1309 (2006).

[7] J. M. Alarcon, V. Lensky and V. Pascalutsa, Eur. Phys. J. C **74**, no. 4, 2852 (2014).

[8] R. Pohl *et al.* Science **353**, Issue 6300, pp. 669-673 (2016)

[9] F. J. Federspiel *et al.*, Phys. Rev. Lett. **67**, 1511 (1991).

[10] A. Zieger *et al.*, Phys. Lett. B **278**, 34 (1992).

[11] B. E. MacGibbon *et al.*, Phys. Rev. C **52**, 2097 (1995).

[12] V. Olmos de Leon *et al.*, Eur. Phys. J. A **10**, 207 (2001).

[13] E. L. Hallin *et al.*, Phys. Rev. C **48**, 1497 (1993).

[14] K. A. Olive et al. (Particle Data Group), Chin. Phys. C, 38, 090001 (2014).

[15] V. Lensky and V. Pascalutsa, Eur. J. Phys. C **65**, 195 (2010).

[16] N. Krupina and V. Pascalutsa, Phys. Rev. Lett. **110**, 262001 (2013).

[17] V. Sokhoyan et al., publication in preparation (under internal review).

[18] J. McGovern, D. Phillips, H. Griesshammer, Eur. Phys. J. C **49**, 12 (2013).

[19] B. Pasquini, D. Drechsel, and M. Vanderhaeghen, Phys. Rev. C **76**, 015203 (2007).

[20] D. Drechsel, M. Gorchtein, B. Pasquini, M. Vanderhaeghen, Phys. Rev. C 61, 015204 (1999).

[21] J.A. McGovern, D.R. Philips, H.W. Griesshammer, Eur. Phys. J. A 49, 12 (2013).

[22] J. C. McGeorge *et al.*, Eur. Phys. J. **A 37**, 129 (2008).

[23] A. Reiter *et al.*, Eur. Phys. J. **A 30**, 461 (2006).

[24] S. Prakhov *et al.*, Phys. Rev. C 79, 035204 (2009).

[25] G. Audit *et al.*, Nucl. Instr. Meth. A 301, 473 (1991).

A Experimental apparatus

A.1 Photon Beam

The A2 photon beam is derived from the production of Bremsstrahlung photons during the passage of the MAMI electron beam through a thin radiator. The resulting photons can be circularly polarised, with the application of a polarised electron beam, or linearly polarised, in the case of a crystalline radiator. The degree of polarisation achieved is dependent on the energy of the incident photon beam (E_0) and the energy range of interest, but currently peaks at ∼75% for linear polarisation (Fig. 6) and ∼85% for circular polarisation (Fig. 7). The maximum degree of linear polarisation should be further improved by 5 to 10% by the end of 2009 when the collimation and beam monitoring systems will be optimised for MAMI-C during the installation of the Frozen Spin Target. The Glasgow-Mainz Photon Tagger (Fig 8) provides energy tagging of the photons by detecting the post-radiating electrons and can determine the photon energy with a resolution of 2 to 4 MeV depending on the incident beam energy, with a single-counter time resolution $\sigma_t = 0.17$ ns [22]. Each counter can operate reliably to a rate of ~ 1 MHz, giving a photon flux of 2.5×10^5 photons per MeV. Photons can be tagged in the momentum range from 4.7 to 93.0% of E_0.

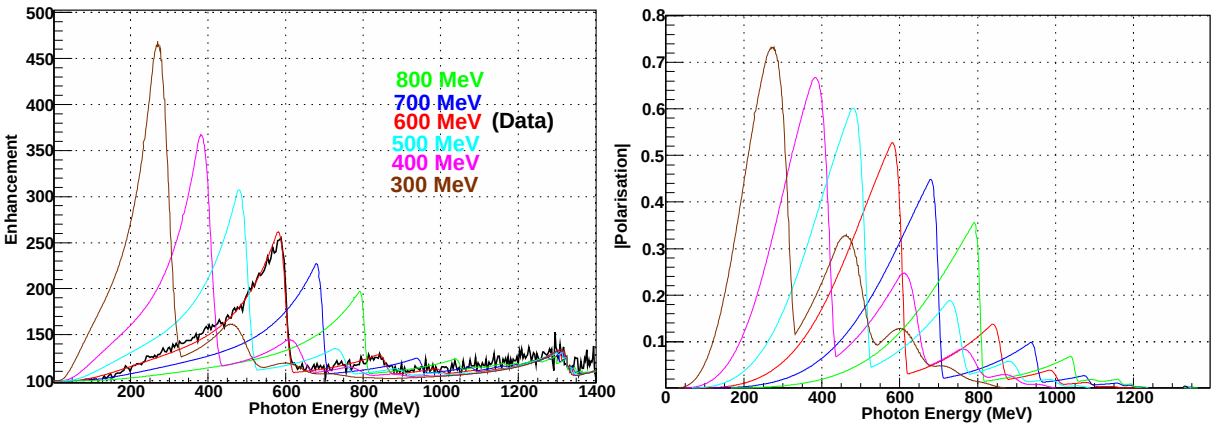

Figure 6: Linear polarisation available with the current collimation system for a variety of crystal orientations. The thin black lines are data obtained during recent MAMI-C runs.

To augment the standard focal plane detector system and make use of the Tagger's intrinsic energy resolution of 0.4 MeV (FWHM), there exists a scintillating fibre detector ("Tagger Microscope") that can improve the energy resolution by a factor of ∼6 for a ∼100 MeV wide region of the focal plane (dependent on its position) [23].

A.2 Crystal Ball Detector System

The central detector system consists of the Crystal Ball calorimeter combined with a barrel of scintillation counters for particle identification and two coaxial multiwire proportional counters for charged particle tracking. This central system provides position, energy and timing information for both charged and neutral particles in the region between 21° and 159° in the polar angle, θ, and over almost the full azimuthal (ϕ) range. At forward angles,

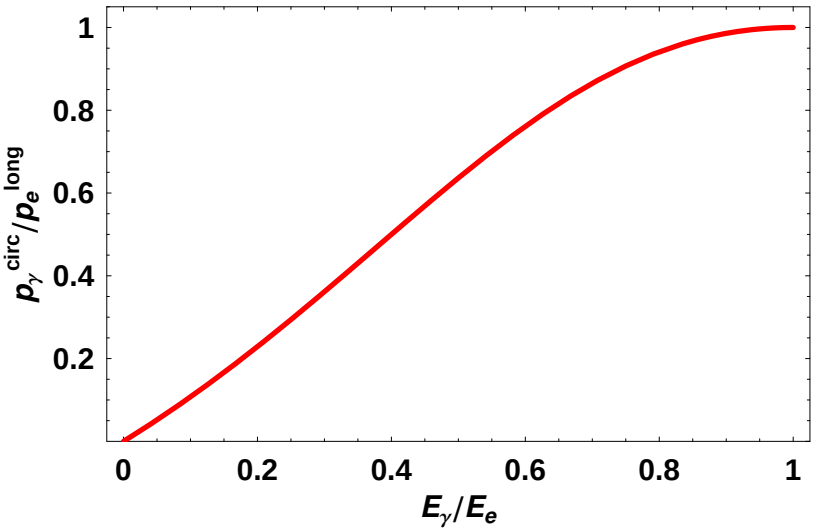

Figure 7: Helicity transfer from the electron to the photon beam as function of the energy transfer. The MAMI beam polarisation is P_e =85%.

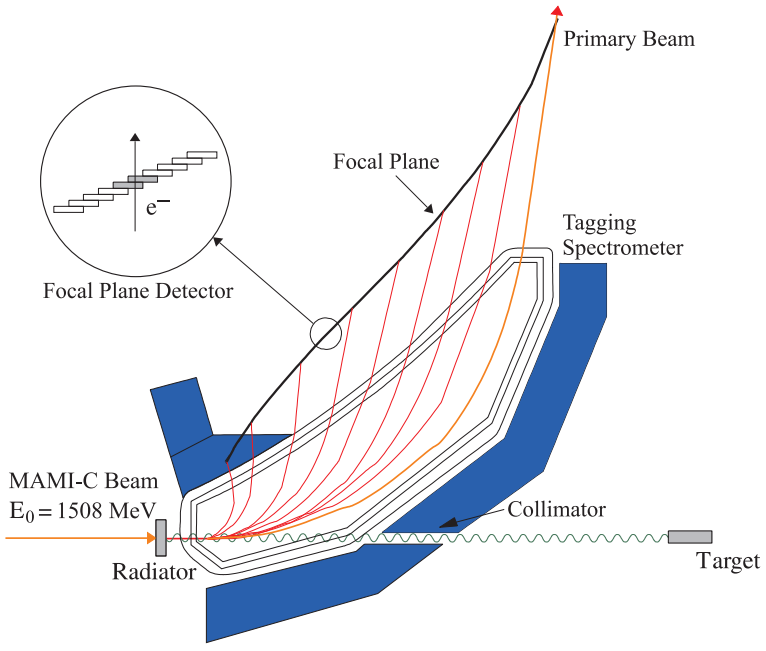

Figure 8: The Glasgow-Edinburgh-Mainz photon tagging spectrometer

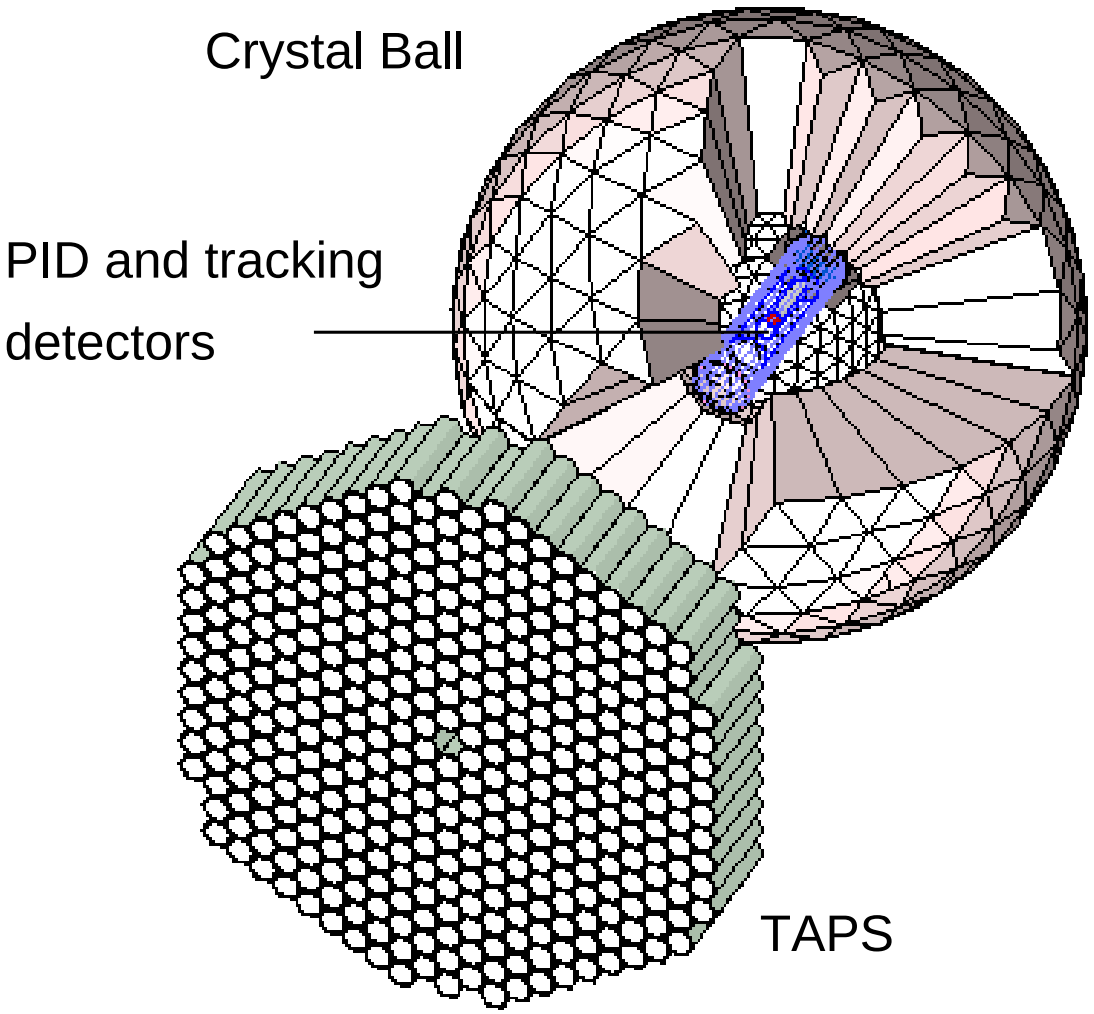

Figure 9: The A2 detector setup: the Crystal Ball calorimeter with cut-away section showing the inner detectors and the TAPS forward wall.

less than 21°, reaction products are detected in the TAPS forward wall. The full, almost hermetic, detector system is shown schematically in Fig. 9 and the measured two-photon invariant mass spectrum is shown in Fig. 10.

The Crystal Ball detector is a highly segmented 672-element NaI(Tl), self triggering photon spectrometer constructed at SLAC in the 1970's. Each element is a truncated triangular pyramid 41 cm (l5.7 radiation lengths) long. The Ball has an energy resolution of $\Delta E/E = 0.020(E[GeV])^{0.36}$, an angular resolution in σ_θ of $2-3°$ and σ_ϕ of $\sigma_\theta/\sin\theta$ for electromagnetic showers [24]. The readout electronics for the Crystal Ball were completely renewed in 2003, and it now is fully equipped with SADCs which allow for the full sampling of pulse-shape element by element. In normal operation, the onboard summing capacity of these ADCs is used to enable dynamic pedestal subtraction and the provision of pedestal, signal and tail values for each element event-by-event. Each CB element is also newly equipped with multi-hit CATCH TDCs. The readout of the CB is effected in such a way as to allow for flexible triggering algorithms. There is an analogue sum of all ADCs, allowing for a total energy trigger, and also an OR of groups of sixteen crystals to allow for a hit-multiplicity second-level trigger—ideal for use when searching for high multiplicity

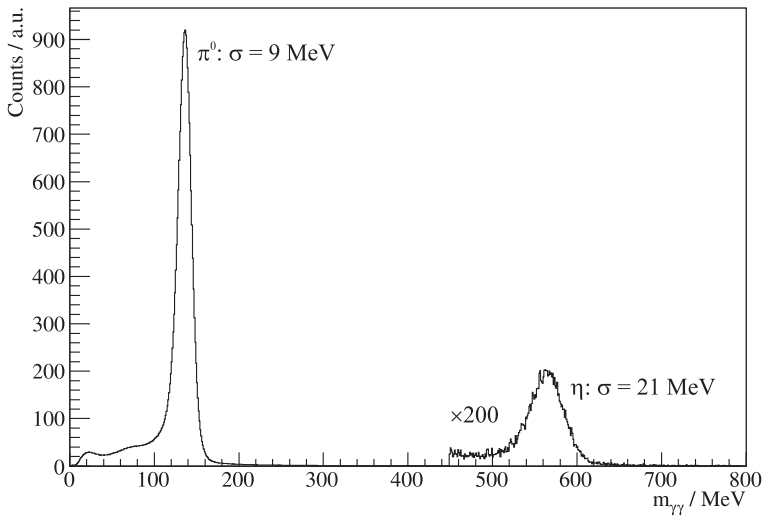

Figure 10: Two gamma invariant mass spectrum for the CB TAPS detector setup. Both η and π^0 mesons can be clearly seen.

final states.

In order to distinguish between neutral and charged particles species detected by the Crystal Ball, the system is equipped with PID 2, a barrel detector of twenty-four 50 mm long 4 mm thick scintillators, arranged so that each PID 2 scintillator subtends an angle of 15° in ϕ. By matching a hit in the PID 2 with a corresponding hit in the CB, it is possible to use the locus of the ΔE, E combination to identify the particle species (Fig. 11). This is primarily used for the separation of charged pions, electrons and protons. The PID 2 covers from 15° to 159° in θ.

The excellent CB position resolution for photons stems from the fact that a given photon triggers several crystals and the energy-weighted mean of their positions locates the photon position to better than the crystal pitch. For charged particles which deposit their energy over only one or two crystals, this is not so precise. Here the tracks of charged particles emitted within the angular and momentum acceptance of the CB detector will be reconstructed from the coordinates of point of intersections of the tracks with two coaxial cylindrical multiwire proportional chambers (MWPCs) with cathode strip readout. These MWPCs are similar to those installed inside the CB during the first round of MAMI-B runs [25]. The most significant difference is that all detector signals are taken at the upstream end of the MWPCs, minimising the material required and facilitating particle detection in the forward polar region.

A mixture of argon (79.5%), ethane (30%) and freon-CF_4 (0.5%) is used as the filling gas. This mixture is a compromise between charge multiplication and localization requirements imposed by the ionizing particle tracks.

Within each chamber both the azimuthal and the longitudinal coordinates of the avalanche will be evaluated form the centroid of the charge distribution induced on the cathode strips. The location of the hit wires(s) will be used to resolve ambiguities which arise from the fact that each pair of inner and outer strip cross each other twice. The expected angular resolution (rms) will be $\approx 2°$ in the polar emission angle ϑ and $\approx 3°$ in the azimuthal emission angle φ.

The MWPCs have been recently installed inside the CB frame and their calibration

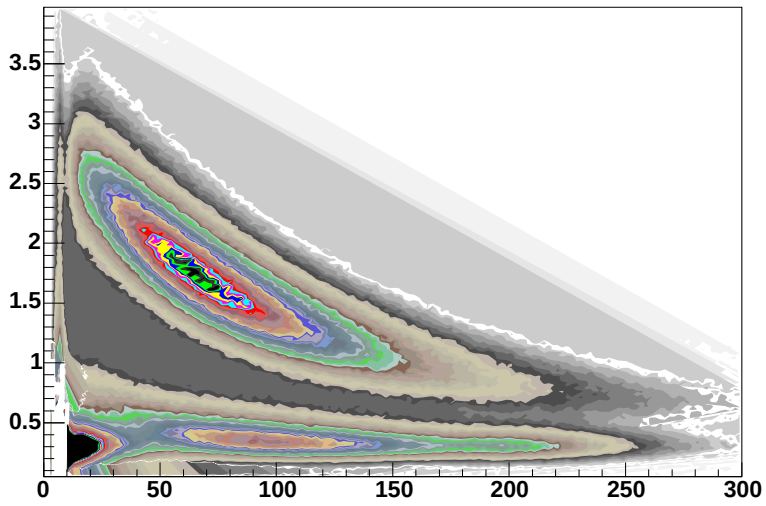

Figure 11: A typical ΔE/E plot from the PID detector. The upper curved region is the proton locus, the lower region contains the pions and the peak towards the origin contains mostly electrons.

using both cosmic rays and test beam data is currently underway.

A.3 TAPS Forward Wall

The TAPS forward wall is composed of 384 BaF_2 elements, each 25cm in length (12 radiation lengths) and hexagonal in cross section, with a diameter of 59 mm. Every TAPS element is covered by a 5 mm thick plastic veto scintillator. The single counter time resolution is $\sigma_t = 0.2$ ns. The energy resolution can be described by the $\Delta E/E = 0.018 + 0.008/(E[GeV])^{0.5}$ [24]. The angular resolution in the polar angle is better than 1°, and in the azimuthal angle it improves with increasing θ, being always better than 1/R radian, where R is the distance in centimeters from the central point of the TAPS wall surface to the point on the surface where the particle trajectory meets the detector. The TAPS readout was custom built for the beginning of the CB@MAMI program and is effected in such a way as to allow particle identification by Pulse-Shape Analysis (PSA), Time-of-Fight (TOF) and ΔE/E methods (using the energy deposit in the plastic scintillator to give ΔE). TAPS can also contribute to the CB multiplicity trigger and is currently divided into upto six sectors for this purpose.